

C(NN)FD - deep learning predictions of tip clearance variations on multi-stage axial compressors aerodynamic performance

Giuseppe Bruni^{a,b,*}, Sepehr Maleki^b, Senthil K. Krishnababu^{a,b}

^aSiemens Energy, 1 Waterside South, Lincoln, LN5 7FD, United Kingdom

^bUniversity of Lincoln, Brayford Way, Lincoln, LN6 7DL, United Kingdom

Abstract

Application of deep learning methods to physical simulations such as CFD (Computational Fluid Dynamics), have been so far of limited industrial relevance. This paper demonstrates the development and application of a deep learning framework for real-time predictions of the impact of tip clearance variations on the aerodynamic performance of multi-stage axial compressors in gas turbines. The proposed *C(NN)FD* architecture is proven to be scalable to industrial applications, and achieves in real-time accuracy comparable to the CFD benchmark. The deployed model, is readily integrated within the manufacturing and build process of gas turbines, thus providing the opportunity to analytically assess the impact on performance and potentially reduce requirements for expensive physical tests.

Keywords:

Aerodynamics, Axial Compressor, CFD, Convolutional Neural Network, Deep Learning, Gas Turbine.

1. Introduction

Gas turbine manufacturers have gathered vast amount of operational data over the years, enabling them to establish best practices and design guidelines for their manufacturing and build processes. These guidelines, often consider a trade-off between cost and engine performance, with tolerance ranges specified accordingly. However, the impact on performance used to define these ranges is typically based on previous experience and simplified correlations. Significant advancements in accuracy and computational cost, have also made CFD analyses an integral part of industrial design processes. Despite these advances, analytical models are generally limited to simplified scenarios (not considering real-world effects). Build-specific CFD models are not traditionally used as part of the manufacturing and build process as a day-to-day occurrence, due to the associated computational cost and requirement for specialized engineers to carry out the analyses. The proposed deep learning framework aims to model the effect of manufacturing and build variations on engine performance, achieving similar accuracies to standard CFD solvers, in a significantly shorter timescale. The focus of the current work is on tip clearance variations, one of the main sources of performance variability, but the framework is readily generalizable to other manufacturing variations. This framework is envisioned to be incorporated into the manufacturing and build process, providing instantaneous feedback,

which can potentially be used to reduce the requirements for expensive physical testing when clearances go outside the acceptance limits.

The challenge: The impact of manufacturing and build variations on the overall performance of gas turbines is known to be significant [1] [2], with the axial compressor, as shown in Figure 1, being a large contributor. For a given design, compressor efficiency is affected by a combination of in-tolerance variations, which can lead to a substantial increase in CO_2 emissions compared to the design target. The aerodynamic performance of multi-stage axial compressors is predicted as standard practice using CFD. These calculations are traditionally performed only for a simplified "as designed" geometry, that differs from the specific build of each engine. Therefore, accurately predicting the impact of manufacturing and build variations on engine performance within a short timescale is of great industrial and environmental importance.

Our contribution: This work demonstrates the development and application of a novel deep learning framework for predicting the impact of manufacturing and build variations on the flow field and overall performance of a multi-stage axial compressors in real-time. Our proposed methodology achieves accuracy levels similar to those of a standard CFD solvers, within a significantly shorter timescale. This work extends the architecture first introduced in previous work by the authors [3], to an application of industrial relevance, demonstrating the aim to provide a generalisable framework. This is integrated into the manufacturing and build process, without incurring the computational costs and specialized personnel required for CFD analyses.

*Corresponding author

Email address: giuseppe.bruni@siemens-energy.com (Giuseppe Bruni)

¹This work was supported and funded by Siemens Energy Industrial Turbo-machinery Ltd.

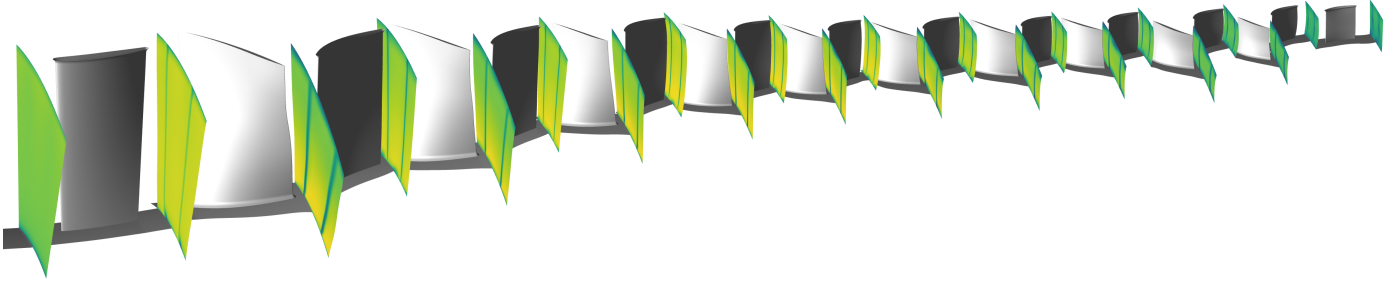


Figure 1: Overview of the CFD domain and axial velocity contours at the mixing-plane locations

1.1. Tip Clearance variation background

The term tip clearance refers to the radial distance between the stationary and rotating components within the compressor, such as the rotor blades and casing, or stator blades and rotor hub. Generally, the tip clearance must be large enough to prevent rubbing during operation, but small enough to avoid excessive aerodynamic losses. Axial compressors are designed to operate at a defined tip clearance, which can vary across stages. During manufacturing, the "cold clearance" is specified and measured as part of the build process in stationary conditions. However, during operation, the "hot clearance" can be significantly smaller due to thermal expansion and centrifugal effects. The cold clearance values have a target value and tolerance range, set by gas turbine manufacturers, based on trade-offs between undesirable rubbing and minimizing tip leakage losses. For a given "cold clearance", the corresponding "hot clearance" can be calculated using either analytical models or operational experience. The "hot clearance" is the actual clearance found during operation, and therefore is used in the CFD and machine learning models presented in this paper. The aerodynamic mechanisms driving tip leakage flows have been extensively researched over the years [4] and can be modeled analytically with varying degrees of fidelity. Steady-state single passage CFD calculations are often used to model the effects of tip clearance variations on overall performance [5], and are used as ground-truth for this study. Non-axisymmetric tip clearance variations are known to affect the overall performance and surge margin [6] and can be relevant for in-service degradation. However, for manufacturing variations they can be neglected [3] and single passage models can be used.

1.2. Machine Learning applications to turbomachinery

In recent years, there has been a significant amount of research into the utilization of machine learning techniques for turbomachinery applications. These include predicting the aerodynamic performance due to tip clearance variations [7] and design modifications [8], as well as aeromechanic predictions for both forced response [9] and flutter [10]. As often the output variables are predicted directly from the input variables with a "black box" approach, these methodologies have varying degrees of accuracy and generalizability, depending on the complexity of the application. However, the ability to accurately predict variations in target variables for turbomachinery in a manner that is both reliable and generalizable, is contingent

upon the accuracy of flow field predictions. It is only through precise flow field predictions that the overall performance figure of interest can be calculated through the application of relevant physical equations that govern the dynamics. The potential benefits of using machine learning approaches for predicting full flow fields, has been demonstrated in some simplified cases in literature for 2D aerofoils on both cartesian [11] and unstructured [12] grids, including novel applications of graph neural network [13] [14]. These methodologies have also been applied to 3D turbomachinery, with a single row compressor [15] and turbine [16], which suggested potential challenges related to scalability and practicality for industrial applications. For instance, the computational cost associated with training, and the size of the required model, make the approach impractical for multi-stage compressors. These applications typically use computational meshes in the order of magnitude of 10 million nodes. Furthermore, storing the CFD data required for training and future simulations would require several petabytes, for a typical engine manufacturer, which is not practical.

1.3. Novel solution to machine learning scalability

To address these challenges, we introduce a pre-processing step to extract only the relevant engineering data from the computational domain, such as blade-to-blade planes, blade surfaces, axial cuts, loading distributions, radial distributions, stage-wise performance, and overall performance. In most cases, these provide sufficient information to the aerodynamicist for design and analyses activities, while close examination of the 3D flow field of a CFD solution is generally only necessary in non-standard cases. Once the relevant engineering data has been extracted from the computational domain, it can be interpolated onto a simplified grid with a resolution that is deemed acceptable for the application in question. Only selected fundamental variables are predicted, while the derived ones can be computed using the appropriate physical equations, significantly reducing the computational cost without sacrificing accuracy, as only the necessary data required to calculate the target variables is retained. This was first introduced by the authors in a previous work for a single stage compressor application [3], and is now extended to a multi-stage compressor application. Later, a similar approach was presented by Li [17], using CNNs to predict the flow field downstream of a single fan row, for noise predictions applications.

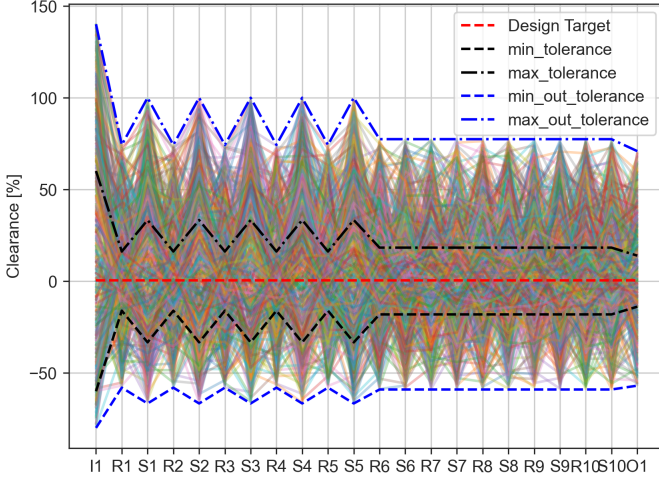


Figure 2: Overview of the tip clearance stage-wise variations in the dataset

2. Methodology

A modern multi-stage industrial axial compressor consisting of 10 stages, as shown in Figure 1, is considered in this work. Each stage is comprised by a row of rotor blades and a row of stator blades with a given blade count. The effect of tip clearance variations on each blade row is the focus of this study. Future work will include other manufacturing and build variations such as surface roughness and geometry variations.

2.1. Data Generation

The ground-truth data used for training are the CFD results for the configuration of interest. This computational model consisted of a single passage model of the 10 stages, with mixing plane interfaces. The computational mesh was generated using Numeca AUTOGRID5, and the CFD solver used was Trace, with SST $K - \omega$ turbulence model. More details on the computational setup used have been provided in previous publications [9]. The tip clearance was varied for each row within the tolerance range first, and then considering out-of-tolerance conditions up to 50% larger and tighter than the drawing specifications, as shown in Figure 2. This range is significantly larger than the tolerance typically specified for gas turbine applications, and was selected to demonstrate the robustness of the methodology to out-of-tolerance cases. The input variable space was sampled using latin-hypercube sampling. The CFD results are processed to only extract five variables, namely, Total Pressure (P_t), Total Temperature (T_t), Axial Velocity (V_x), Tangential Velocity (V_t), and Density (ρ), at each of the 24 inter-row locations as shown in Figure 1. Previous work [3] also considered Radial Velocity (V_r), which is neglected in this work, to reduce the computational cost, as we found it to have no impact on the performance predictions. The flow condition at each mesh node is fully described by the five variables and can be used to calculate all other available flow variables in the CFD solution. While the CFD mesh for each simulation comprises over 15 million nodes, the post-processed domain contains less

than 100 thousand nodes overall, yet it includes all the necessary information for the desired engineering assessment. This consists only of the 24 inter-row 2D planes with a 64×64 grid. The data is stored as a tensor with a channel-first convention and a shape of $(5 \times 24 \times 64 \times 64)$, where the dimensions represent the number of variables, number of axial locations, tangential nodes in the mesh, and radial nodes in the mesh, respectively. Although the present study focuses solely on a single compressor geometry and operating point, the variation in tip clearance has a significant impact on the flow field. To reduce the computational cost of the CFD analysis, rotational periodicity can be assumed, and only a single passage needs to be considered instead of the full annulus. Typically, 2D contours are only used for detailed analyses, whereas mass-flow averaging [18] in the circumferential direction is more commonly used to obtain radial profiles of the variables of interest for most engineering applications. These radial profiles of each variable are then mass-flow averaged [18] to obtain a 1D average, which is used to calculate stage-wise performance of the variables of interest, such as pressure-ratio (PR), and polytropic efficiency (η_p). In addition to the aerodynamic performance of the stage, it is possible to calculate the overall performance of the compressor. Predicting the stage-wise performance in addition to the overall performance is critical for implementation of the model in the gas turbine build process, as it provides detailed information on which blade rows should be targeted by corrective measures.

2.2. The $C(NN)FD$ framework

An overview of the framework for a multistage compressor application, is shown in Figure 3. The tip clearance values and relevant geometry design parameters of a specific build are fed as input to $C(NN)FD$, which predicts the 2D contours for all variables at the locations of interest. The outputs are mass-flow averaged to obtain the relevant radial profiles and 1D averages, which are then used to calculate stage-wise performance first, and then the overall performance using relevant thermodynamic equations. As the impact of tip clearance variations depends on the aerodynamic loading distribution of a given aerofoil, the methodology should be generalizable to different designs. Therefore, $C(NN)FD$ requires the geometries associated with each clearance value as input. This is achieved by considering a series of design parameters to describe the geometry of each blade, such as stagger angle, camber angle, maximum thickness, etc. Since we consider only a single compressor design, the geometry parameters are fixed. In future work we will investigate the effect of geometrical variations and different designs. The architecture shown in Figure 4, is a variant of the one originally proposed by the authors in previous work [3]. The model is based on a U-Net architecture, incorporating 3D convolutions and residual connections for each convolutional block. The encoding section followed by the decoding section, along with the skip connections, enables the network to predict both low-level and high-level features in the flow field. The use of residual connections improves convergence and makes this type of architecture scalable to larger models required for full compressor applications.

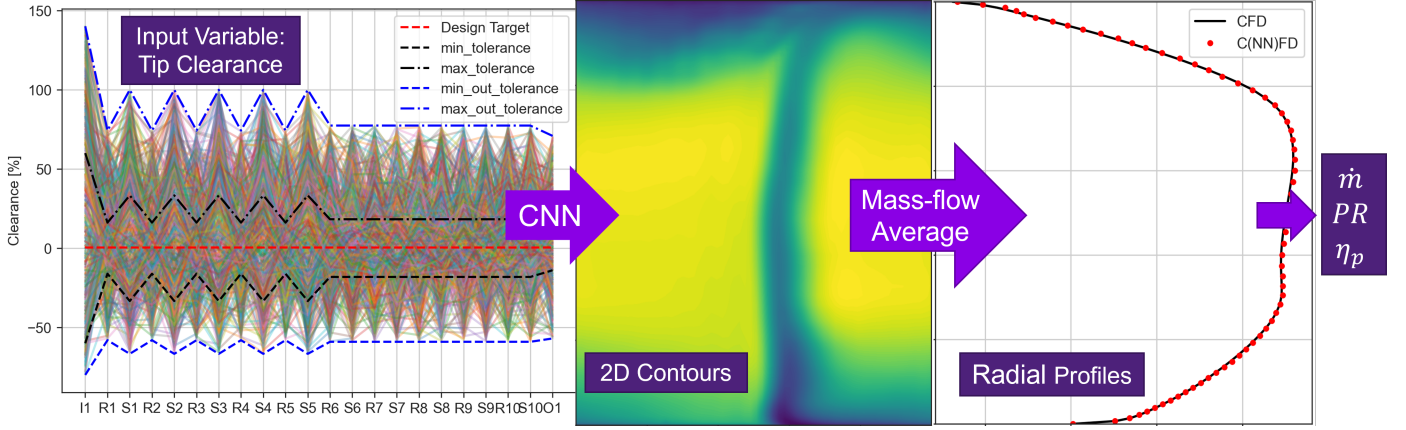


Figure 3: C(NN)FD framework overview

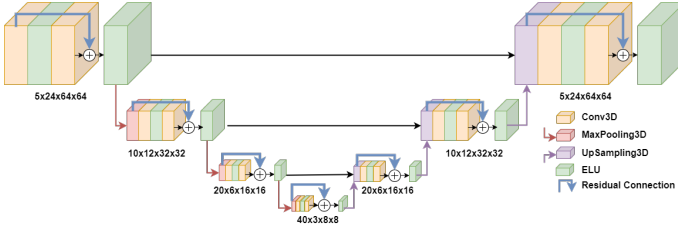


Figure 4: C(NN)FD architecture overview

The first input of the network is a tensor with the tip clearance values of size (22×1) , representing respectively the number of rows, and the tip clearance values. The second input is a tensor with the blade geometry design parameters of size $(22 \times 8 \times 5)$, which represent the number of rows, number of radial sections, and number of design variables. The two tensors are then added and duplicated to match the dimensions required by the U-Net input of $(5 \times 24 \times 64 \times 64)$. The output of the network is a tensor of size $(5 \times 24 \times 64 \times 64)$, which encompasses the entire flow field. The width of the network is limited to three down-sampling steps due to the selected max-pooling operation's stride of $(2, 2, 2)$, resulting in a bottleneck section with tensors of shape $(40 \times 3 \times 8 \times 8)$. Batch Normalization is implemented before each convolutional layer, and the activation function employed for all layers is *ELU*. The network is trained using the *AdamW* optimizer, with *Huber* loss function. The training time for a new model from scratch is around 3 hours on a single Tesla K80 GPU. This is reduced to less than 1 hour when re-training the network when data becomes available, thus making the architecture scalable for industrial applications. The execution time for inference is less than 1 second, making the predictions of the deployed model effectively real-time for the application of interest. The selected architecture was found to be the best performing in comparison to a series of fully connected and convolutional neural networks that were considered during development. The dataset generated for this study comprises 300 CFD solutions, each of which was executed using automated and parallelized processes, taking 90 minutes on 72 CPUs for each case. Even if the computational

cost required to generate the dataset for supervised training is potentially high, it should be noted that most of the data is already available from internal work of the industrial partner. It is envisioned that the majority of the data used for training of this framework will be based on available data, with additional computations carried out only when required, to extend the dataset for wider generalizability. The dataset was divided into three sets: 70% training data, 20% validation data, and 10% hold-out data. The validation set was utilized to evaluate model performance and perform hyper-parameter tuning, while the hold-out set was reserved only for a final assessment. This ensures that the results are generalisable to unseen cases, and will lead to comparable performance also when deployed in a production environment.

3. Results

In this section, the predicted flow field generated by *C(NN)FD* is compared to the CFD ground truth for the worst case scenario, where the largest discrepancy between the two was found in the hold-out set. All values presented are non-dimensionalized with respect to the results obtained from the nominal clearance baseline. The *Span [%]* y-axis represents the radial direction in the gas path, ranging from the hub surface at the bottom to the casing surface at the top. The θ [%] x-axis represents the circumferential direction in the gas path, with a range between 0 and 1 representing one passage. Each row corresponds to a specific number of blades, and thus the gas path can be divided into a number of passages equal to the blade count. A comparison between the ground truth on the left and the predictions on the right provides an overview of the flow field differences.

The results are presented in Figure 5, Figure 7 and Figure 9 for Stage-1, Stage-5 and Stage-10 Axial Velocity only. The relative error between the ground truth and the predictions at each mesh node are shown in Figure 6, Figure 8 and Figure 10 for Axial Velocity V_x at Stage-1, Stage-5 and Stage-10. All the other stages and variables exhibit similar level of agreement and are not presented for conciseness. The predictions generated by *C(NN)FD* exhibit excellent agreement with

the ground truth, with the primary flow features being accurately reproduced. Only minor differences are observed in regions with high gradients, but well within the numerical uncertainty of the CFD solver. Due to operational requirements, the aerodynamic design of axial compressor leads to greatly different flow features across the different stages. For instance, front stages tend to operate at transonic conditions, with strong shock-waves interacting with the tip leakage flows. Conversely, the rear stages are subsonic, with the flow field dominated by end-wall flow features. The proposed architecture is demonstrated to be able to predict the flow field within the compressor for both transonic and subsonic stages, even with significantly different flow features as seen for instance by comparing Figure 5 and Figure 9. The highest local error is in the order of magnitude of 0.1%, which is well within the numerical error of the CFD solver. The errors are generally localised to regions with steep gradients and to only few nodes in the mesh, being therefore effectively negligible.

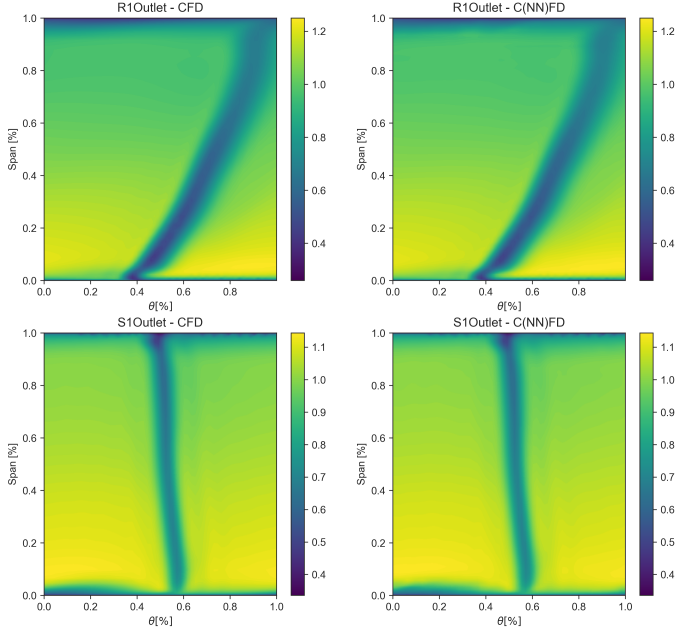


Figure 5: Stage 1 V_x contours - CFD and ML predictions comparison

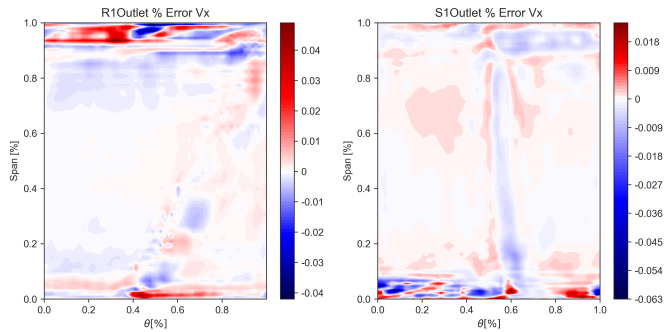


Figure 6: Stage 1 2D contours % error between CFD and ML predictions

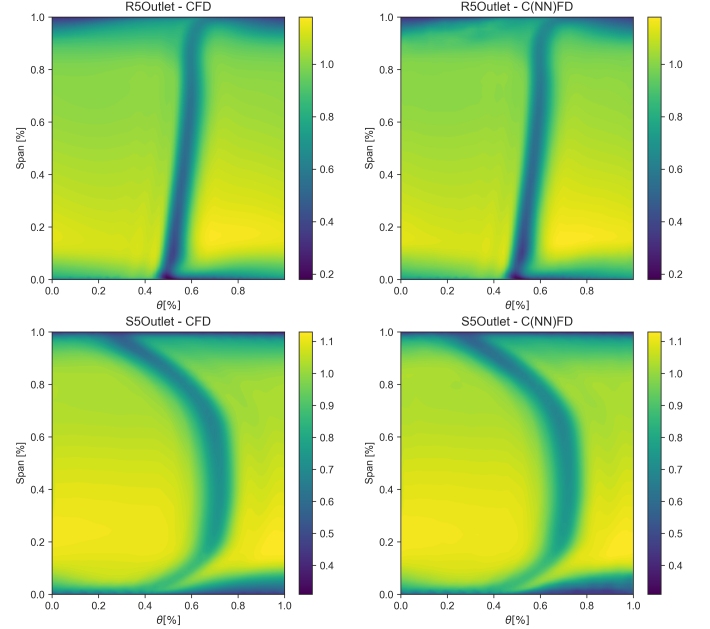


Figure 7: Stage 5 V_x contours - CFD and ML predictions comparison

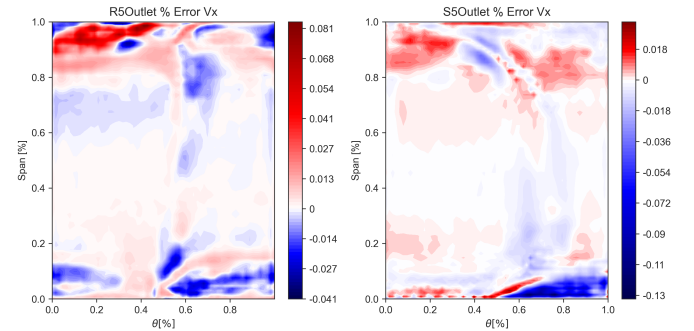


Figure 8: Stage 5 2D contours % error between CFD and ML predictions

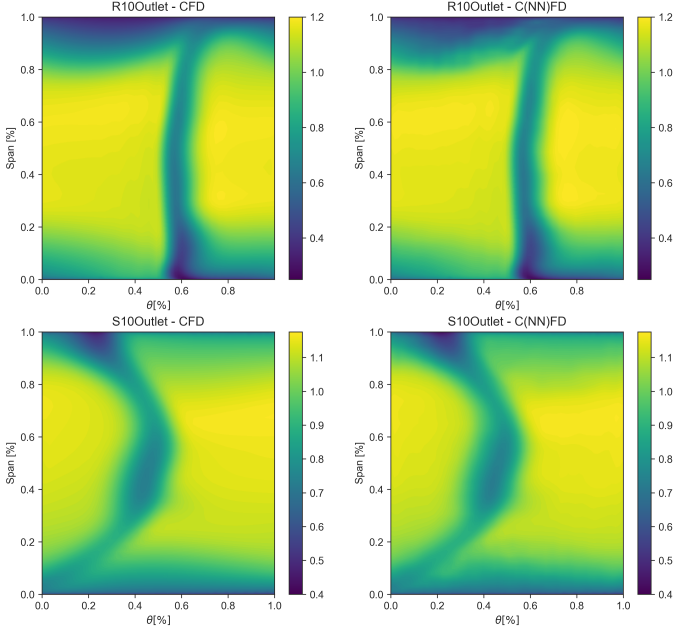


Figure 9: Stage 10 V_x contours - CFD and ML predictions comparison

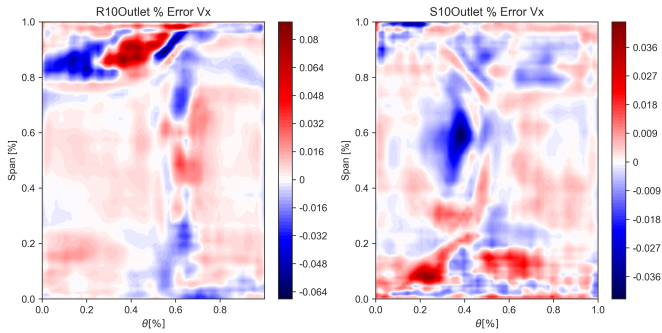


Figure 10: Stage 10 2D contours % error between CFD and ML predictions

When performing mass-flow averaging to obtain the radial profiles, the discrepancies between the ground truth and predictions are even less significant. Figure 11, Figure 12 and Figure 13 indicate that the radial profiles for $C(NN)FD$ and CFD are effectively overlapping. It is notable how even the end-wall regions, characterized by steep gradients, are well-resolved by $C(NN)FD$. This confirms that the localized errors in the 2D contours prediction do not significantly affect the results for the radial profiles.

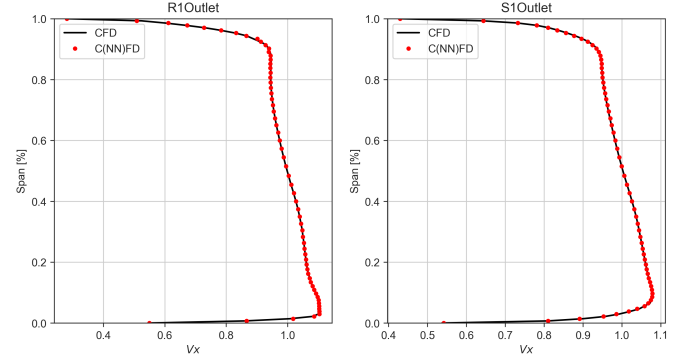


Figure 11: Radial profiles comparison between ground truth and predicted values - Stage 1

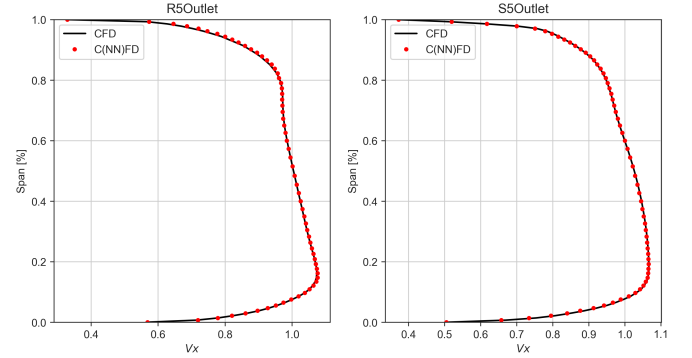


Figure 12: Radial profiles comparison between ground truth and predicted values - Stage 5

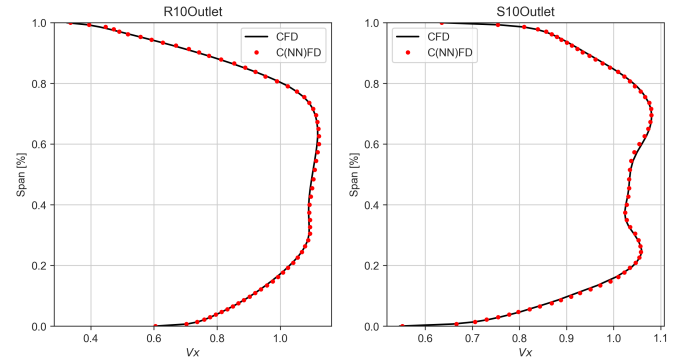


Figure 13: Radial profiles comparison between ground truth and predicted values - Stage 10

The radial profiles are then mass-flow averaged to obtain the relevant 1D averages, which are utilized to compute the stage-wise performance as shown in Figure 17 and Figure 18, as well as the overall performance variables of interest in Figure 14 and Figure 15. Predicting the stage-wise performance in addition to the overall performance is critical for implementation of the model in the gas turbine build process, as it provides detailed information on which blade rows should be targeted by corrective measures. An excellent agreement is observed for all overall performance parameters, with a coefficient of determination R^2 close to 1 for all variables. This indicates that the proposed model can accurately describe most of the variance present in the dataset. Moreover, the Mean-Absolute-Error for each variable is smaller than the known uncertainties of the CFD ground truth results and significantly smaller than the dataset's range.

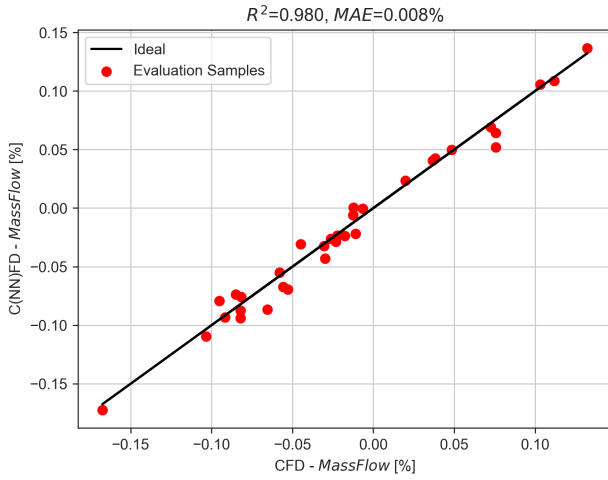


Figure 14: Comparison between predicted (C(NN)FD) and ground truth (CFD) values: Mass-flow

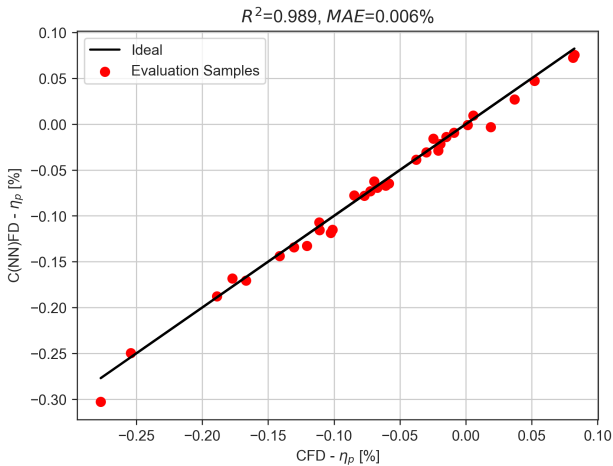


Figure 15: Comparison between predicted (C(NN)FD) and ground truth (CFD) values: Polytropic Efficiency

The $C(NN)FD$ predictions remain accurate even for the case with the lowest efficiency in the hold-out set, demonstrating the model's capability to handle challenging aerodynamic conditions typical of large clearances. The largest discrepancy is found for the case with the lowest efficiency in the hold-out set, which shows a difference of less than 0.03 percentage points in overall efficiency. This discrepancy is negligible for overall performance predictions, and demonstrates how the proposed architecture reliably predicts even the most challenging cases. This is a particularly challenging case aerodynamically, as very large and very tight clearances are alternated in the front stages of the compressor, as shown in Figure 16. This would result in strong tip leakage flows leading to high losses and low efficiency in the blade rows with large clearances. Those would affect the downstream blade rows with tight clearance, whose potentially high efficiency will be affected by the unfavorable upstream conditions, leading to complex inter-row interactions and stage re-matching. The discrepancy between predictions and ground truth discussed for the overall performance is more noticeable in the stage-wise distribution of Figure 17 and Figure 18. While C(NN)FD predicts the trend for each stage, relative to the baseline, for Stages 1, 2, 3 and 6 the variation relative to the baseline is slightly over-predicted for both beneficial and detrimental effects. The predictions could potentially be improved by providing more training data including those extreme clearance combinations, where it was deemed relevant from an industrial perspective.

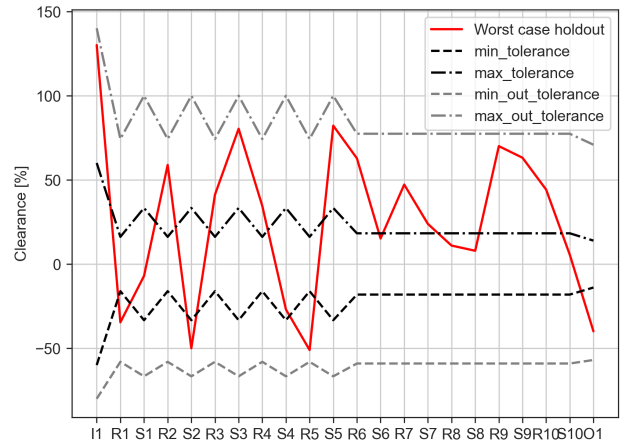


Figure 16: Stagewise clearance distribution for worst case in the hold-out set

4. Deployment to manufacturing and build process

The accuracy of the framework that we propose has been proven on the hold-out set, and was therefore deemed to acceptable for deployment to a production environment. This is then demonstrated by applying the pipeline to 4 different engine builds, providing an example of application to the manufacturing and build process, as well as the associated conclusions and actions that can be taken based on the results of the C(NN)FD real-time predictions. The results were also later verified using CFD, showing an error in the overall efficiency predictions of less than 0.01 percentage points for all the cases. The cold clearances for the 4 engine builds of interest were converted to hot clearance based on operational experience, and an overview of the hot clearance distribution compared to the tolerance range is provided in Figure 19. The overall performance predictions in Figure 20 show that the impact of those tip clearance variations on performance compared to the baseline is negligible.

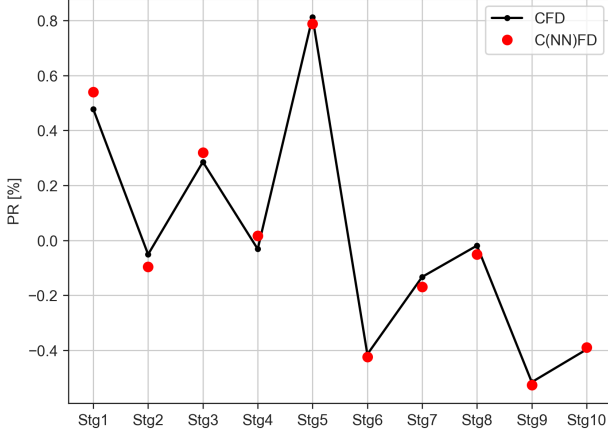


Figure 17: Comparison between predicted (C(NN)FD) and ground truth (CFD) values for worst case in the hold-out set: PR Stage-wise distribution

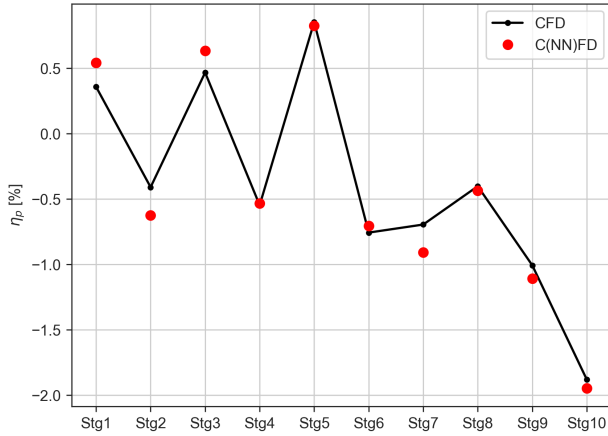


Figure 18: Comparison between predicted (C(NN)FD) and ground truth (CFD) values for worst case in the hold-out set: η_p Stage-wise distribution

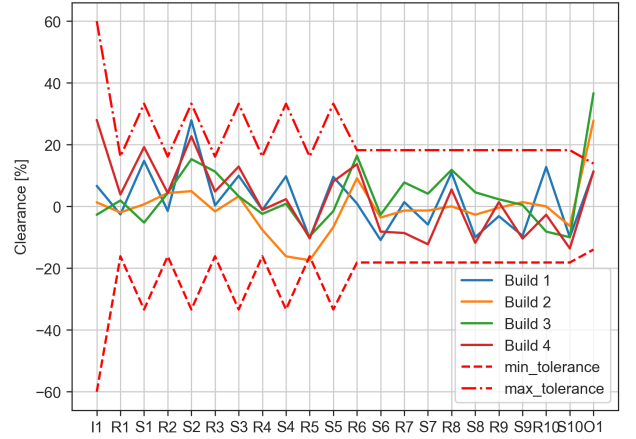


Figure 19: Variation in hot clearance of different builds

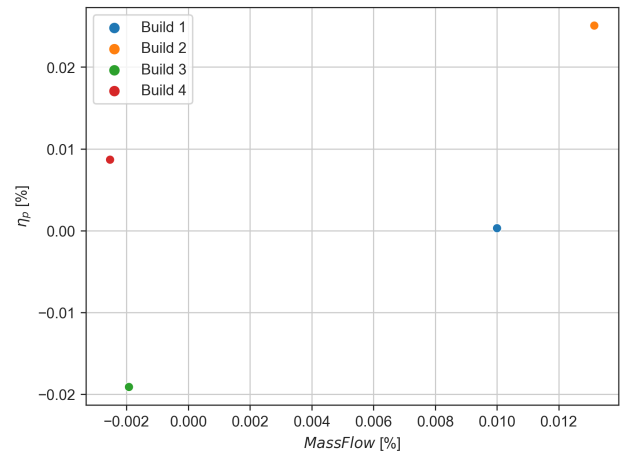


Figure 20: Overall Performance Predictions of different builds

It can be noted that most of the rows have clearances within the specified tolerance for all the builds, with the exception of O1 for Build 2 and 3. Moreover, a large clearance close to the tolerance limit is found for S2 in Build 1 and 4, as well as R6 for Build 3 and 4. Build 3 is found to be the worst performer compared to the baseline, with a drop of $-0.02[\%]$ in polytropic efficiency and $-0.002[\%]$ in mass flow. Therefore, the manufacturing non-conformance could potentially be deemed acceptable, as the out-of-tolerance clearance for O1 does not significantly affect the overall performance. Increased O1 clearance could also potentially affect the compressor exit diffuser performance, which will also be considered in future work. In addition to overall performance, C(NN)FD can also provide real time predictions of the stage-wise distributions, as shown in Figure 21 and Figure 22. In Figure 19, large clearances close to the tolerance limit were identified for S2 in Build 1 and 4, as well as R6 for Build 3 and 4. Based on the efficiency stage-wise distributions, S2 is found to have a minor impact on Stage-2 and Stage-3, as the neighboring rows have tight clearance which compensate for it. R6 on the other hand is found to have a much more significant impact on Stage-6 efficiency, which drops by more than $-0.2[\%]$ for Build 4. However, this is compensated by the rear stages which have tighter clearances, leading to higher stage efficiency. Build 3 was found to provide the lowest overall efficiency, due to a drop in stage efficiency for Stage-3, 6, 7 and 8. When targeting an efficiency improvement for Build 3, it would be necessary to improve the clearance for S2, R3, R6, R7, S7, R8 and S8 as they were found to have larger than design clearance, driving the reduction in stage efficiency. This demonstrates how C(NN)FD can be used as a predictive tool to assess the performance of a given engine build, without the need for computationally expensive CFD analysis, and potentially avoiding re-testing for engines which would not meet the contractual performance requirements. Moreover, this tool can be used for a selective build process, where different parts available in stock can be selected based on the expected overall performance. The focus of this work was on compressor performance at design points conditions, while future work will extend the assessment to more off-design conditions and surge margin predictions.

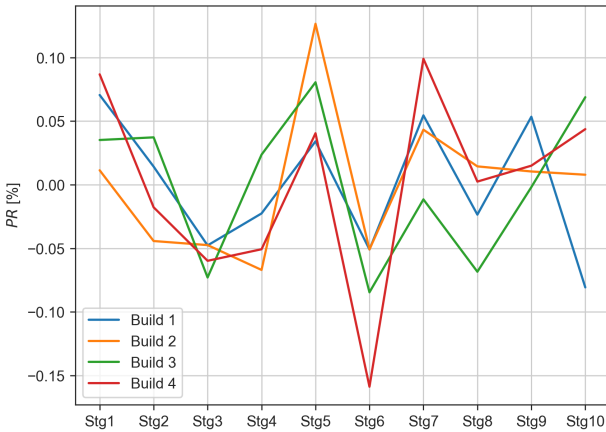


Figure 21: Stage-wise PR distribution of different builds

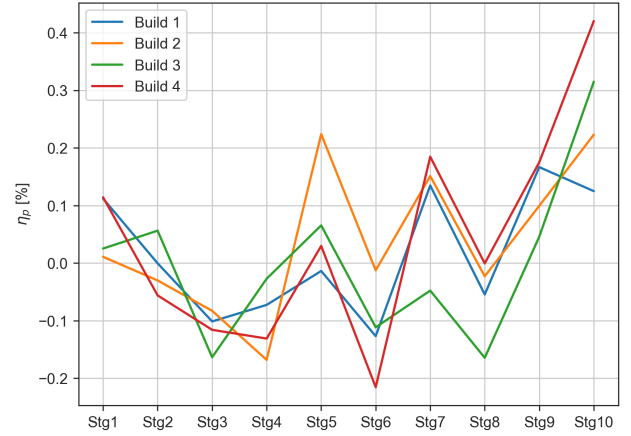


Figure 22: Stage-wise η_p distribution of different builds

5. Conclusion

This study presents the development and application of a novel deep learning framework for real-time predictions of the impact of tip clearance variations on the flow field and overall performance of multi-stage axial compressors. The proposed C(NN)FD architecture achieves real-time accuracy comparable to the CFD benchmark. Our methodology is generalizable because of the flow field predictions, which are utilized to calculate the corresponding stage-wise and overall performance. Our methodology is also scalable to industrial applications because of physics-based selective use of relevant parts of the CFD solution. The deployed model, is envisioned to be integrated within the manufacturing and build process of gas turbines, thus providing the opportunity to analytically assess the impact on performance and to take the appropriate measures to potentially avoid repeating expensive physical tests and CO_2 emissions.

References

- [1] F. Montomoli, Uncertainty quantification in computational fluid dynamics and aircraft engines: Second edition, Springer International Publishing, 2018. doi:10.1007/978-3-319-92943-9. URL <https://doi.org/10.1007/978-3-319-92943-9>
- [2] J. Wang, X. Zheng, Review of Geometric Uncertainty Quantification in Gas Turbines, Journal of Engineering for Gas Turbines and Power 142 (7) (06 2020). doi:10.1115/1.4047179. URL <https://doi.org/10.1115/1.4047179>
- [3] G. Bruni, S. Maleki, S. K. Krishnababu, C(nn)fd - a deep learning framework for turbomachinery cfd analysis (2023). arXiv:2306.05889.
- [4] J. A. Storer, N. A. Cumpsty, Tip Leakage Flow in Axial Compressors, Journal of Turbomachinery 113 (2) (1991) 252–259. doi:10.1115/1.2929095. URL <https://doi.org/10.1115/1.2929095>
- [5] S. Sakulkaew, C. S. Tan, E. Donahoo, C. Cornelius, M. Montgomery, Compressor Efficiency Variation With Rotor Tip Gap From Vanishing to Large Clearance, Journal of Turbomachinery 135 (3) (03 2013). doi:10.1115/1.4007547. URL <https://doi.org/10.1115/1.4007547>
- [6] V. Suriyanarayanan, Q. Rendu, M. Vahdati, L. Salles, Effect of Manufacturing Tolerance in Flow Past a Compressor Blade, Journal of Turbomachinery 144 (4) (11 2021). doi:10.1115/1.4052600. URL <https://doi.org/10.1115/1.4052600>

- [7] S. Krishnababu, O. Valero, R. Wells, AI Assisted High Fidelity Multi-Physics Digital Twin of Industrial Gas Turbines, Vol. Volume 2D of Turbo Expo: Power for Land, Sea, and Air, 2021. doi:10.1115/GT2021-58925.
URL <https://doi.org/10.1115/GT2021-58925>
- [8] J. Pongetti, T. Kipouros, M. Emmanuelli, R. Ahlfeld, S. Shahpar, Using Autoencoders and Output Consolidation to Improve Machine Learning Models for Turbomachinery Applications, Vol. Volume 2D of Turbo Expo: Power for Land, Sea, and Air, 2021. doi:10.1115/GT2021-60158.
URL <https://doi.org/10.1115/GT2021-60158>
- [9] G. Bruni, S. Krishnababu, S. Jackson, Application of Machine Learning to Forced Response Predictions of an Industrial Axial Compressor Rotor Blade, Journal of Engineering for Gas Turbines and Power 145 (1) (10 2022). doi:10.1115/1.4055634.
URL <https://doi.org/10.1115/1.4055634>
- [10] X. He, M. Rauseo, Q. Rendu, L. Salles, M. Vahdati, F. Zhao, Turbomachinery aerodynamic and aeroelastic predictions with machine learning, 16th International Symposium on Unsteady Aerodynamics Aeroacoustics and Aeroelasticity of Turbomachines, 2022.
- [11] N. Thuerey, K. Weißenow, L. Prantl, X. Hu, Deep learning methods for reynolds-averaged navier-stokes simulations of airfoil flows, AIAA Journal 58 (1) (2020) 25–36. doi:10.2514/1.J058291.
URL <https://doi.org/10.2514/1.J058291>
- [12] A. Kashefi, D. Rempe, L. J. Guibas, A point-cloud deep learning framework for prediction of fluid flow fields on irregular geometries, Physics of Fluids 33 (2) (02 2021). doi:10.1063/5.0033376.
URL <https://doi.org/10.1063/5.0033376>
- [13] L. Harsch, S. Riedelbauch, Direct prediction of steady-state flow fields in meshed domain with graph networks, International Conference on Learning Representations, 2021.
URL <https://doi.org/10.48550/arXiv.2105.02575>
- [14] T. Pfaff, M. Fortunato, A. Sanchez-Gonzalez, P. Battaglia, Learning mesh-based simulation with graph networks, International Conference on Learning Representations, 2021.
URL <https://doi.org/10.48550/arXiv.2010.03409>
- [15] K. Beqiraj, A. Perrone, M. Sanguineti, L. Ratto, G. Ricci, Rotor37 Aerodynamic Optimization: A Machine Learning Approach, Vol. Volume 10D of Turbo Expo: Power for Land, Sea, and Air, 2022. doi:10.1115/GT2022-83063.
URL <https://doi.org/10.1115/GT2022-83063>
- [16] J. Li, T. Liu, Y. Wang, Y. Xie, Integrated graph deep learning framework for flow field reconstruction and performance prediction of turbomachinery, Energy 254 (2022) 124440. doi:<https://doi.org/10.1016/j.energy.2022.124440>
URL <https://doi.org/10.1016/j.energy.2022.124440>
- [17] N. Li, J. Winkler, C. A. Reimann, D. Voytovych, M. Joly, K. G. Lore, J. Mendoza, S. M. Grace, Machine learning aided fan broadband interaction noise prediction for leaned and swept fans, in: AIAA AVIATION 2023 Forum. doi:10.2514/6.2023-4297.
URL <https://arc.aiaa.org/doi/abs/10.2514/6.2023-4297>
- [18] N. A. Cumpsty, J. H. Horlock, Averaging Nonuniform Flow for a Purpose, Journal of Turbomachinery 128 (1) (2005) 120–129. doi:10.1115/1.2098807.
URL <https://doi.org/10.1115/1.2098807>